

Determination of  $\gamma$  from the  $\eta - \eta'$  mixing within QCD Factorization

Prasanta Kumar Das \*

The Institute of Mathematical Sciences,  
C.I.T Campus, Taramani, Chennai-600113, India.

**Abstract**

The charmless nonleptonic  $B \rightarrow \eta K$  decay is an useful probe to test the strong interaction dynamics part of the Standard Model. Within the QCD factorization framework, we analyse this particular decay by using the most recent data of  $BR(B^+ \rightarrow \eta K^+)$  and  $A_{cp}(B^+ \rightarrow \eta K^+)$  available in the Heavy Flavour Averaging Group (HFAG) website. Using these data we constraint the unitarity angle  $\gamma$  and  $\eta - \eta'$  mixing angle  $\theta$ . We find that such constraint is scale dependent, e.g. for  $\gamma = 70^\circ$ , the data for  $BR(B^+ \rightarrow \eta K^+)$  ( $= (2.6 \pm 0.5) \times 10^{-6}$ ) suggests that  $\theta$  should lie in between  $-46^\circ$  and  $-44^\circ$ ,  $-30^\circ$  and  $-26^\circ$  for  $\mu = m_b/2$ . For  $\mu = m_b$ , the same  $BR$  data (with the same  $\gamma$ ) suggests that  $\theta$  should lie in between  $-54^\circ$  and  $-50^\circ$ ,  $-30^\circ$  and  $-26^\circ$ . The allowed region followed from  $A_{cp} = -0.25 \pm 0.14$ , is found to be rather wider than that obtained from the  $BR(B^+ \rightarrow \eta K^+)$  data. For  $\gamma = 70^\circ$  and  $\theta = -21.3^\circ$ , we find  $BR(B^-(+) \rightarrow \eta K^-(+)) = 2.93(4.91) \times 10^{-6}$  and  $A_{cp} = -0.252$  at  $\mu = m_b$ , and about  $2.98(5.72) \times 10^{-6}$  and  $-0.315$  corresponding to  $\mu = m_b/2$ . We investigate the role of the power corrections in such constraints.

*Keywords:* B-meson; QCD; Factorization.

*PACS Nos.:* 14.40.Nd; 12.38.Aw; 12.39.St.

---

\*E-mail: dasp@imsc.res.in

# 1 Intrduction

The nonleptonic weak hadronic decays of the  $B$  meson is an useful probe to test the Standard Model(SM), particularly the dynamics of it's strong interaction (QCD) part. Due to the non-perturbative features, the amplitudes for such hadronic  $B$ -decays, are difficult to calculate directly from the QCD lagrangian. For the phenomenological study, several factorization hypotheses, like naive-factorization(NF), generalized factorization(GF) and QCD factorization(QCDF) were introduced and has been quite successful in explaining the data for exclusive  $B$  decays, like  $B \rightarrow PP, PV, VV, PT, VT$  (where  $P, V$  and  $T$  stands for pseudoscalar, vector and tensor meson) reported by the CLEO, BABAR and BELLE collaborations [1, 2, 3]. Out of all these hypothesis, the QCD factorization hypothesis [4] particularly, has become very much popular in recent years because of it's successful explanation of the several  $B$  factories data. Studying the nonleptonic  $B^{-(+)} \rightarrow \eta K^{-(+)}$  decay within the QCD factorization, exploring it's CP-violation aspects, is a well motivated topic and is the main concern of the present work.

The only source of the CP violation in the Standard Model(SM) is the CKM matrix  $V_{CKM}$  [5], which is arised due to the misalignment of the mass and weak interaction eigenstates. It is expressed via the charge current-current interaction lagrangian  $\mathcal{L}_{int}^{CC}$ , defined by

$$\mathcal{L}_{int}^{CC} = -\frac{g}{\sqrt{2}} \begin{pmatrix} \bar{u}_L & \bar{c}_L & \bar{t}_L \end{pmatrix} \gamma_\mu V_{CKM} \begin{pmatrix} d_L \\ s_L \\ b_L \end{pmatrix} W_\mu^+ + h.c. \quad (1)$$

In the Wolfenstein parametrization  $V_{CKM}$  is given by

$$V_{CKM} = \begin{pmatrix} V_{ud} & V_{us} & V_{ub} \\ V_{cd} & V_{cs} & V_{cb} \\ V_{td} & V_{ts} & V_{tb} \end{pmatrix} = \begin{pmatrix} 1 - \frac{1}{2}\lambda^2 & \lambda & A\lambda^3(\rho - i\eta) \\ -\lambda & 1 - \frac{1}{2}\lambda^2 & A\lambda^2 \\ A\lambda^3(1 - \rho - i\eta) & -A\lambda^2 & 1 \end{pmatrix} + \mathcal{O}(\lambda^4), \quad (2)$$

where  $\lambda = V_{us} = \sin\theta_c$ ,  $\theta_c$ , the Cabibbo mixing angle. The angle  $\gamma$  related to the phase of the CKM element  $V_{ub}$  i.e.  $\gamma = \arg(V_{ub}^*)$  (which follows from  $V_{ub} = |V_{ub}|e^{-i\gamma} = A\lambda^3(\rho - i\eta)$ ), amounts to CP violation in the SM. The angle  $\gamma$  is one of the three angles  $\alpha, \beta$  and  $\gamma$  of the unitarity triangle and any nonzero value of it (resulting into non zero area of the unitarity triangle) yields the CP violation in the SM. Hence, a precise measurement of the unitarity angle  $\gamma$  can be possible from the CP violating transition, which is being considered in the present work. There exist bounds on the angle  $\gamma$  and one such bound is followed from the time-dependent CP asymmetry  $S_{\pi\pi}$  measurement. The current average experimental value of the  $S_{\pi\pi}$  which is about  $-0.49 \pm 0.27$ , yields [6]

$$\gamma = (66_{-16}^{+19})^\circ \quad \text{or} \quad (174_{-8}^{+9})^\circ, \quad (3)$$

where both set of solutions are consistent with each other and the first set is consistent with the unitarity-triangle fit. Our next concern is the mixing angle  $\theta$  between the psedoscalar  $\eta$  and  $\eta'$  mesons, a matter of great interst from the time when the  $SU(3)$  flavour symmetry was proposed. In the simplest scenario where the  $\eta$  and  $\eta'$  mesons do not mix with other pseudoscalar mesons, like excited quarkonium states, gluonium or exotics, the  $\eta, \eta'$  wave functions can be written as

$$|\eta\rangle = \cos\theta |\eta_8\rangle - \sin\theta |\eta_0\rangle, \quad (4)$$

$$|\eta'\rangle = \sin\theta |\eta_8\rangle + \cos\theta |\eta_0\rangle, \quad (5)$$

where the  $SU(3)$  basis states  $|\eta_8\rangle$  and  $|\eta_0\rangle$  are given by

$$|\eta_8\rangle = \frac{1}{\sqrt{6}}|u\bar{u} + d\bar{d} - 2s\bar{s}\rangle, \quad (6)$$

$$|\eta_0\rangle = \frac{1}{\sqrt{3}}|u\bar{u} + d\bar{d} + s\bar{s}\rangle. \quad (7)$$

From the accumulated data of the decay widths  $\Gamma[\eta \rightarrow \gamma\gamma] = (0.46 \pm 0.04) \text{ KeV}$ ,  $\Gamma[\eta' \rightarrow \gamma\gamma] = (4.26 \pm 0.19) \text{ KeV}$  and  $\Gamma[\pi^0 \rightarrow \gamma\gamma] = (7.7 \pm 0.55) \text{ eV}$ , one finds [7],

$$\theta = -21.3^\circ \pm 2.5^\circ. \quad (8)$$

In the present analysis we will treat the unitarity angle  $\gamma$  and mixing angle  $\theta$  as the unknown parameters and use the most recent data for the direct CP asymmetry  $A_{cp}(B^+ \rightarrow \eta K^+)$  and  $BR(B^+ \rightarrow \eta K^+)$  [8] to put constraints on them.

The organization of the paper is as follows. Section 2 begins with the general discussion of the nonleptonic decay of a  $B$  meson within the QCD factorization framework, which includes the discussion of several non-factorizable corrections, e.g. vertex, penguin, hard-spectator and the weak annihilation corrections. They are present in the QCD factorization framework, but absent in the simplest naive factorization(NF) framework. We obtain the SM decay amplitude  $\mathcal{M}_{SM}(B^+ \rightarrow \eta K^+)$ ,  $BR(B^+ \rightarrow \eta K^+)$  and  $A_{cp}(B^+ \rightarrow \eta K^+)$ . Section 3 is fully devoted to the numerical analysis. After describing several numerical inputs i.e. the CKM matrix elements, effective coefficients, quarks masses, decay constants, form factors, we discuss the constraints in the  $\theta - \gamma$  contour plane, which is being obtained by using the most recent data of  $BR(B^+ \rightarrow \eta K^+)$  and  $A_{cp}(B^+ \rightarrow \eta K^+)$ , available in the HFAG website [8]. In Section 4, we summarize our results and made our conclusion.

## 2 $B^- \rightarrow \eta K^-$ decay within the QCDF framework:

The most general effective weak Hamiltonian  $\mathcal{H}_{\text{eff}}^{\Delta B=1}$  for the non-leptonic  $\Delta B = 1$  transitions can be expressed via the operator product expansion (OPE) [10]

$$\mathcal{H}_{\text{eff}} = \frac{G_F}{\sqrt{2}} \left[ V_{ub}V_{us}^* (c_1 O_1^u + c_2 O_2^u) + V_{cb}V_{cs}^* (c_1 O_1^c + c_2 O_2^c) - V_{tb}V_{ts}^* \left( \sum_{i=3}^{10} c_i O_i \right) \right] + \text{H.c.} \quad (9)$$

Here  $c_i$ 's are the wilson coefficients and the 4-quarks current-current, gluonic and electroweak penguin operators are defined by

- **current-current operators:**

$$\begin{aligned} O_1^u &= (\bar{u}b)_{V-A}(\bar{s}u)_{V-A} & O_2^u &= (\bar{u}_\alpha b_\beta)_{V-A}(\bar{s}_\beta u_\alpha)_{V-A}, \\ O_1^c &= (\bar{c}b)_{V-A}(\bar{s}c)_{V-A} & O_2^c &= (\bar{c}_\alpha b_\beta)_{V-A}(\bar{s}_\beta c_\alpha)_{V-A}, \end{aligned} \quad (10)$$

- **QCD-penguin operators:**

$$\begin{aligned} O_3 &= (\bar{s}b)_{V-A} \sum_q (\bar{q}q)_{V-A}, & O_4 &= (\bar{s}_\alpha b_\beta)_{V-A} \sum_q (\bar{q}_\beta q_\alpha)_{V-A}, \\ O_5 &= (\bar{s}b)_{V-A} \sum_q (\bar{q}q)_{V+A}, & O_6 &= (\bar{s}_\alpha b_\beta)_{V-A} \sum_q (\bar{q}_\beta q_\alpha)_{V+A}, \end{aligned} \quad (11)$$

- **electroweak-penguin operators:**

$$\begin{aligned} O_7 &= \frac{3}{2}(\bar{s}b)_{V-A} \sum_q e_q (\bar{q}q)_{V+A}, & O_8 &= \frac{3}{2}(\bar{s}_\alpha b_\beta)_{V-A} \sum_q e_q (\bar{q}_\beta q_\alpha)_{V+A}, \\ O_9 &= \frac{3}{2}(\bar{s}b)_{V-A} \sum_q e_q (\bar{q}q)_{V-A}, & O_{10} &= \frac{3}{2}(\bar{s}_\alpha b_\beta)_{V-A} \sum_q e_q (\bar{q}_\beta q_\alpha)_{V-A}, \end{aligned} \quad (12)$$

where  $\alpha, \beta$  are the  $SU(3)$  color indices,  $V \pm A$  correspond to  $\gamma^\mu(1 \pm \gamma^5)$  and the wilson coefficients  $c_i$ 's, in which the QCD correction to weak interaction is encoded, are evaluated at the scale  $\mathcal{O}(\mu \simeq m_b)$ .  $e$  and  $g$  are respectively QED and QCD coupling constants and  $T^a$ 's are  $SU(3)$  color matrices. For the penguin operators,  $O_3, \dots, O_{10}$ , the sum over  $q$  runs over different quark flavors, active at  $\mu \simeq m_b$ , i.e.  $q \in \{u, d, s, c, b\}$ . Note that the gluonic penguin operators  $O_{3-6}$  contributes largely to  $B \rightarrow \eta K$ . The contributions coming from the electroweak penguin operators are not so significant and will be neglected in the present analysis.

The wilson coefficients  $c_i$ s, quite well-known at the NLO order accuracy, is evaluated at  $\mu \simeq m_b$  and is within the perturbative control. The nontriviality (amounting uncertainty) exists in the evaluation of

the hadronic matrix elements of the operators in the effective Hamiltonian comprising  $B \rightarrow \eta K$  transition. Several approximations are made in order to have a control over this. Within naive factorization framework, one assumes the absence of the order  $\mathcal{O}(\alpha_s)$  QCD correction to the hadronic matrix element and the validity of working in the heavy quark limit (i.e.  $m_b \gg \Lambda_{QCD}$ ). Within the naive factorization, the hadronic matrix of a  $B$  meson decay to a pair of mesons  $M_1$  and  $M_2$  can be factorized and be written as the product of two quarks bilinear currents  $j_1$  and  $j_2$

$$\langle M_1 M_2 | O_i | \bar{B} \rangle_{NF} = \langle M_1 | j_1 | \bar{B} \rangle \times \langle M_2 | j_2 | 0 \rangle \quad (13)$$

which gives rise the transition form factor and the decay constant, respectively. The operators  $O_i$ , constituting the effective Hamiltonian, is specific to a particular  $B$  decay. In the present case they are represented by Eqns. (10,11,12). Corrections to the naive factorization arises from the “non-factorizable”  $\mathcal{O}(\alpha_s)$  QCD correction to the hadronic matrix element by means of vertex, penguin, hard-spectator and as well as the weak annihilation contributions. The “QCD factorization” framework, which can be looked as the order  $\mathcal{O}(\alpha_s)$  corrected version of the naive factorization framework, encodes all these  $\mathcal{O}(\alpha_s)$  corrections to the hadronic matrix element (13). Within QCD factorization, the above two body nonleptonic decay amplitude (Eqn. (13), in the heavy quark limit, can be generalized as [4]

$$\begin{aligned} \langle M_1 M_2 | O_i | \bar{B} \rangle_{QCDF} &= \sum_j F_j^{B \rightarrow M_1}(m_2^2) \int_0^1 du T_{ij}^I(u) \Phi_{M_2}(u) + (M_1 \leftrightarrow M_2) \\ &+ \int_0^1 d\xi du dv T_i^{II}(\xi, u, v) \Phi_B(\xi) \Phi_{M_1}(v) \Phi_{M_2}(u) \end{aligned} \quad (14)$$

where  $M_1$  and  $M_2$  corresponds to the light mesons. The factor  $F^{B \rightarrow M_1(M_2)}$  corresponds to the  $B \rightarrow M_1$  transition form factor, while the  $\Phi_X$  corresponds to the Light Cone Distribution Amplitudes (LCDA) for the meson  $X$  for the quark-antiquark Fock states. The perturbatively calculable quantities  $T_{ij}^{I,II}$  in Eqn. (14), which are known as the hard-scattering kernels, contain essentially the  $\mathcal{O}(\alpha_s)$  QCD correction to the matrix element.  $T_{ij}^I$  which starts at  $\mathcal{O}(\alpha_s^0)$ , corresponds to the vertex, penguin correction, while  $T_{ij}^{II}$  which starts at  $\mathcal{O}(\alpha_s^1)$  corresponds to the hard-spectator correction which arises due to the exchange of a hard gluon between the spectator quark inside the  $\bar{B}$  meson with the quark of the emitted  $M_2$  meson. Note that the weak annihilation contribution are not shown here, we will present them later separately. Now no QCD correction implies the vanishing of the second term of Eqn. (14), while  $T_{ij}^I$  turns into a constant. After performing the relevant integration (Eqn. (14)) with the leading twist-2 LCDA's, one in the heavy quark limit ends up a expression, which much looks like: **form factor**  $\times$  **decay constnt**, agrees with the naive factorization result (Eqn. (13)). Following the above discussion, the generic  $\bar{B} \rightarrow M_1 M_2$  decay amplitude, in the heavy quark limit  $m_b \gg \Lambda_{QCD}$  within the QCDF framework, can be written as

$$\langle M_1 M_2 | O_i | \bar{B} \rangle_{QCDF} = \langle M_1 M_2 | O_i | \bar{B} \rangle_{NF} \left[ 1 + \sum_n r_n \alpha_s^n + \mathcal{O}\left(\frac{\Lambda_{QCD}}{m_b}\right) \right]. \quad (15)$$

Note that in the heavy quark limit ( $m_b \gg \Lambda_{QCD}$ ) and at order  $\mathcal{O}(\alpha_s)$ , although the naive factorization framework breaks down (due to the presence of the second term), one can still calculates the the corrections systemetically by finding the corresponding corrections in the short-distance coefficients and the LCDA's of the mesons.

In the QCDF framework, the amplitude for the  $\bar{B} \rightarrow \eta K$  can be expressed as

$$\mathcal{M}_{SM}(\bar{B} \rightarrow \eta K) = \mathcal{M}_{SM}^f(\bar{B} \rightarrow \eta K) + \mathcal{M}_{SM}^a(\bar{B} \rightarrow \eta K), \quad (16)$$

where

$$\mathcal{M}_{SM}^f(\bar{B} \rightarrow \eta K) = \frac{G_F}{\sqrt{2}} \sum_{p=u,c} \sum_{i=1}^{i=6} l_p a_i^p \langle \eta K | O_i | \bar{B} \rangle_{NF}, \quad (17)$$

$$\mathcal{M}_{SM}^a(\bar{B} \rightarrow \eta K) = \frac{G_F}{\sqrt{2}} f_B f_K f_\eta \sum_{p=u,c} \sum_{i=1}^{i=6} l_p b_i. \quad (18)$$

In above  $l_p = V_{pb} V_{ps}^*$  with  $V$ 's being the CKM matrix elements,  $G_F$ , the Fermi decay constant, while  $f_r$  ( $r = B, K, \eta, \eta'$ ) stands for the meson decay constants. The non-factorizable vertex, penguin and hard spectator corrections are encoded in the effective coefficients  $a_i^p$  which appeared in the first term of the amplitude (Eqn. (16)). The effective coefficients  $a_i^p$  at the next-to-leading order in  $\alpha_s(\mu)$  takes the following form (for a generic nonleptonic  $\bar{B} \rightarrow M_1 M_2$  decay) [6]

$$a_i^p(M_1, M_2) = \left( c_i(\mu) + \frac{c_{i\pm 1}(\mu)}{N_c} \right) + \frac{c_{i\pm 1}(\mu)}{N_c} \frac{C_F \alpha_s(\mu)}{4\pi} \left[ V_i(M_2) + \frac{4\pi^2}{N_c} H_i(M_1, M_2) \right] + P_i^p(M_2), \quad (19)$$

where  $c_i(\mu)$ , the wilson coefficients with  $i(=1, \dots, 6)$  is odd(even), the upper(lower) sign is applied and for the current-current operator the superscript  $p$  is to be dropped (to avoid confusion). Here  $N_c = 3$  is the colour factor,  $C_F = \frac{N_c^2 - 1}{2N_c}$ , the quadratic Casimir Invariant for  $SU(N)$  ( $N = N_c = 3$  here) and  $c_i$ 's are the wilson coefficients. The quantities  $V_i$ ,  $H_i$  and  $P_i^p$  respectively stands for the “non-factorizable” vertex, hard spectator and penguin corrections and their complete expressions can be found in [4],[6]. The hard spectator functions reads as

$$H_i(K\eta) = \frac{f_B f_K f_\eta^u}{m_B^2 F_0^{B \rightarrow K}(0) f_\eta^u} \int_0^1 \frac{d\xi}{\xi} \Phi_B(\xi) \int_0^1 dx \int_0^1 dy \left[ \frac{\Phi_\eta(x) \Phi_K(y)}{\bar{x}\bar{y}} + r_\chi^K \frac{\Phi_\eta(x) \Phi_K^{(3)}(y)}{x\bar{y}} \right] \quad (20)$$

for  $i = 1-4$ ,

$$H_i(K\eta) = \frac{-f_B f_K f_\eta^u}{m_B^2 F_0^{B \rightarrow K}(0) f_\eta^u} \int_0^1 \frac{d\xi}{\xi} \Phi_B(\xi) \int_0^1 dx \int_0^1 dy \left[ \frac{\Phi_\eta(x) \Phi_K(y)}{x\bar{y}} + \frac{\Phi_\eta(x) \Phi_K^{(3)}(y)}{\bar{x}\bar{y}} \right] \quad (21)$$

for  $i = 5$  with and  $H_i(M_1 M_2) = 0$  for  $i = 6$ . In above  $\bar{j} = 1 - j$  ( $j = x, y$ ) and the term  $r_\chi^K = \frac{2m_K^2}{m_b(\mu)(m_q + m_s)(\mu)}$ , (where  $m_q$  corresponds to the average of the up and down quark masses) is the chiral enhancement factor. The  $\Phi_X(\Phi_X^{(3)})$  corresponds to twist-2 (twist-3) LCDA's of the meson  $X$ . The weak annihilation contribution's  $b_i$ 's corresponding to Eqn. (18), can be expressed as (following [4],[6])

$$b_1 = \frac{C_F}{N_c^2} c_1 A_1^i, \quad b_3^p = \frac{C_F}{N_c^2} [c_3 A_1^i + c_5 (A_3^i + A_3^f) + N_c c_6 A_3^f], \quad (22)$$

$$b_2 = \frac{C_F}{N_c^2} c_2 A_1^i, \quad b_4^p = \frac{C_F}{N_c^2} [c_4 A_1^i + c_6 A_2^i]. \quad (23)$$

where  $b_1, b_2$  corresponds to the current-current annihilation, while  $b_3^p, b_4^p$ , the gluon penguin annihilation. Here  $A_3^f$  is the factorizable annihilation amplitude which is being induced from the  $(S - P) \times (S + P)$  type operators, whereas the non-factorizable annihilation amplitudes  $A_{1,2,3}^i$  are induced from the  $(V - A) \times (V - A)$ ,  $(V + A) \times (V + A)$  and  $(S - P) \times (S + P)$  type operators. Their explicit expressions, which can be found in [4],[6], reads as

$$\begin{aligned} A_1^i &= \pi \alpha_s(\mu) \int_0^1 dx dy \left\{ \Phi_{M_2}(x) \Phi_{M_1}(y) \left[ \frac{1}{y(1-x\bar{y})} + \frac{1}{\bar{x}^2 y} \right] + r_\chi^{M_1} r_\chi^{M_2} \Phi_{M_2}^{(3)}(x) \Phi_{M_1}^{(3)}(y) \frac{2}{\bar{x}y} \right\}, \\ A_1^f &= 0, \\ A_2^i &= \pi \alpha_s(\mu) \int_0^1 dx dy \left\{ \Phi_{M_2}(x) \Phi_{M_1}(y) \left[ \frac{1}{\bar{x}(1-x\bar{y})} + \frac{1}{\bar{x}y^2} \right] + r_\chi^{M_1} r_\chi^{M_2} \Phi_{M_2}^{(3)}(x) \Phi_{M_1}^{(3)}(y) \frac{2}{\bar{x}y} \right\}, \\ A_2^f &= 0, \\ A_3^i &= \pi \alpha_s(\mu) \int_0^1 dx dy \left\{ r_\chi^{M_1} \Phi_{M_2}(x) \Phi_{M_1}^{(3)}(y) \frac{2\bar{y}}{\bar{x}y(1-x\bar{y})} - r_\chi^{M_2} \Phi_{M_1}(y) \Phi_{M_2}^{(3)}(x) \frac{2x}{\bar{x}y(1-x\bar{y})} \right\}, \\ A_3^f &= \pi \alpha_s(\mu) \int_0^1 dx dy \left\{ r_\chi^{M_1} \Phi_{M_2}(x) \Phi_{M_1}^{(3)}(y) \frac{2(1+\bar{x})}{\bar{x}^2 y} + r_\chi^{M_2} \Phi_{M_1}(y) \Phi_{M_2}^{(3)}(x) \frac{2(1+y)}{\bar{x}y^2} \right\}, \end{aligned} \quad (24)$$

for a generic  $\bar{B} \rightarrow M_1 M_2$  decay. In our case of interest, the corresponding expressions are obtained by setting  $M_1 = K(\eta)$  and  $M_2 = \eta(K)$ . Note that the power suppressed twist-3 LCDA  $\Phi_X^{(3)}$  of the hard spectator and annihilation contributions suffers from the end point divergence  $X_{H,A} = \int_0^1 \frac{dy}{y}$ , which can be phenomenologically parametrized as [6]

$$X_H = \int_0^1 \frac{dy}{y} = (1 + \rho_{H,A} e^{i\phi_{H,A}}) \ln \left( \frac{m_B}{\Lambda_h} \right) \quad (25)$$

where  $\Lambda_h \sim 0.5$  GeV,  $\rho_{H,A}$  are free parameters expected to be about of order  $\rho_{H,A} \simeq \mathcal{O}(1)$  and  $\phi_{H,A} \in [0, 2\pi]$ . With all these QCD corrections in hand, we are now ready to give the  $\mathcal{O}(\alpha_s)$  corrected expressions for the  $\bar{B} \rightarrow \eta K$  decay amplitude (i.e. Eqn. (17)) and within QCDF they reads (for  $\bar{B} = B^-$ ) as [7]

$$\begin{aligned} \mathcal{M}_{SM}^f(B^- \rightarrow \eta K^-) = & \frac{G_F}{\sqrt{2}} \left\{ V_{ub} V_{us}^* \left[ a_2^p + a_1^p \frac{m_B^2 - m_\eta^2}{m_B^2 - m_K^2} \frac{F_0^{B \rightarrow \eta}(m_K^2)}{F_0^{B \rightarrow K^-}(m_\eta^2)} \frac{f_K}{f_\eta} \right] + V_{cb} V_{cs}^* a_2^p \frac{f_\eta^c}{f_\eta^u} \right. \\ & - V_{tb} V_{ts}^* \left[ 2a_3^p - 2a_5^p + \left( a_3^p - a_5^p + a_4^p + \frac{a_6^p m_\eta^2}{m_s(m_b - m_s)} \right) \frac{f_\eta^s}{f_\eta^u} - \frac{a_6^p m_\eta^2}{m_s(m_b - m_s)} \right. \\ & \left. \left. + \left( a_4^p + \frac{2a_6^p m_K^2}{(m_s + m_u)(m_b - m_u)} \right) \frac{m_B^2 - m_\eta^2}{m_B^2 - m_K^2} \frac{F_0^{B \rightarrow \eta}(m_K^2)}{F_0^{B \rightarrow K^-}(m_\eta^2)} \frac{f_K}{f_\eta} \right] \right\} \langle K^- | \bar{s} b_- | B^- \rangle \langle \eta | \bar{u} u_- | 0 \rangle \end{aligned} \quad (26)$$

where  $b_-$  (and  $u_-$ ) corresponds to  $\gamma_\mu(1 - \gamma_5)b$  (and  $\gamma_\mu(1 - \gamma_5)u$ ). The transition form factor and decay constants are defined as

$$\begin{aligned} \langle K^-(p') | \bar{s} \gamma^\mu b | B^-(p) \rangle &= \langle K^-(p') | \bar{s} \gamma^\mu b | B^-(p) \rangle \\ &= \left[ \left\{ (p + p')^\mu - \frac{m_B^2 - m_K^2}{q^2} q^\mu \right\} F_1^{B \rightarrow K}(q^2) + \frac{m_B^2 - m_K^2}{q^2} q^\mu F_0^{B \rightarrow K}(q^2) \right] \end{aligned} \quad (27)$$

$$\langle \eta(q) | \bar{u} u_- | 0 \rangle = -\langle \eta(q) | \bar{u} \gamma_\mu \gamma_5 u | 0 \rangle = i f_\eta^u q_\mu. \quad (28)$$

where  $m_B$ ,  $m_K$  corresponds to  $B, K$  mesons masses and  $f_\eta^u$ , the  $\eta$  meson decay constant.  $F_{0,1}^{B \rightarrow K}(q^2)$  are the  $B \rightarrow K$  transition form factors evaluated at  $q^2 = m_\eta^2$ . Note that in the effective coefficients  $a_i^p$  (Eqn. (19)) appearing in the above amplitude (Eqn. (26)) contains the non-factorizable vertex ( $V_i$ ) and penguin ( $P_i^p$ ) corrections, which are evaluated at  $\mu = m_b$  ( $m_b/2$ ) and the hard spectator ( $H_i$ ) and annihilation corrections (given by Eqn. (22)), evaluated at  $\mu = \mu_h \sim \sqrt{\mu \Lambda_h}$ , where  $\Lambda_h \simeq 0.5$  GeV [6]. It is now straightforward to write down the branching ratio (BR) for the  $B^- \rightarrow \eta K^-$  decay as

$$BR(B^- \rightarrow \eta K^-) = \frac{\tau_B p_c}{8\pi m_B^2} |\mathcal{M}(B^- \rightarrow \eta K^-)|^2 \quad (29)$$

where  $\mathcal{M}(B^- \rightarrow \eta K^-)$  is the decay amplitude,  $\tau_B$ , the  $B$  meson life time and  $p_c$ , the c.m. momentum of the  $\eta$  and  $K^-$  mesons in the  $B^-$  rest frame, is given by

$$p_c = \frac{\sqrt{(m_B^2 - (m_\eta - m_{K^-})^2)(m_B^2 - (m_\eta + m_{K^-})^2)}}{2m_B}. \quad (30)$$

The BR's  $BR(B^+ \rightarrow \eta K^+)$  is obtained from  $BR(B^- \rightarrow \eta K^-)$  by performing the relevant changes under CP transformations. The CP-asymmetry  $A_{cp}$ , according to the standard convention, is defined as

$$A_{cp} = \frac{\Gamma(B^- \rightarrow \eta K^-) - \Gamma(B^+ \rightarrow \eta K^+)}{\Gamma(B^- \rightarrow \eta K^-) + \Gamma(B^+ \rightarrow \eta K^+)}. \quad (31)$$

Table 1: Data for the  $B^+ \rightarrow \eta K^+$  decay mode. The error bars are at  $1\sigma$  limit; the upper limit at 90% CL. For  $A_{cp}$  we follow the standard convention as mentioned in the text.

Final State	$BR \times 10^6$	$A_{cp}$
$\eta K^+$	$2.6 \pm 0.5$	$-0.25 \pm 0.14$

### 3 Numerical Analysis

The BR and CP-asymmetry  $A_{cp}$  data for the  $B^+ \rightarrow \eta K^+$  decay are available in the HFAG05 website [8] and is given in Table 1. The decay amplitudes depend on the effective coefficients  $a_i$ 's, CKM matrix elements, quark masses and the non-perturbative inputs like hadronic form factors, decay constants etc.

#### 3.1 CKM matrix elements

The parameters  $A, l, \rho$  and  $\eta$  of the CKM matrix  $V_{CKM}$  (2) in the Wolfenstein parametrization are set at the following values. We employ  $A$  and  $l = \sin \theta_c$  at the values of 0.815 and 0.2205 in our analysis. The other parameters are found to be  $\rho = \sqrt{\bar{\rho}^2 + \bar{\eta}^2} \cos \gamma$  and  $\eta = \sqrt{\bar{\rho}^2 + \bar{\eta}^2} \sin \gamma$  with  $\gamma = \arg(V_{ub}^*)$  (an unknown parameter in our analysis) and  $\sqrt{\bar{\rho}^2 + \bar{\eta}^2} = 0.3854[9]$ . Here  $\bar{\rho} = \rho(1 - \frac{\lambda^2}{2})$  and  $\bar{\eta} = \eta(1 - \frac{\lambda^2}{2})$  [10].

#### 3.2 Effective coefficients $a_i$ , quark masses, decay constants and form factors

The NLO wilson coefficients in the NDR scheme, obtained in the paper by Beneke *et al.* [6], are cataloged in Table 2. The effective coefficients  $a_i$ 's ( $i = 1, 2, \dots, 10$ ) in Eqn.(26), can be obtained by using Eqn.(19) from

Table 2:  $\Delta B = 1$  wilson coefficients at  $\mu = \frac{m_b}{2}(m_b) \sim 2.1(4.2)$  GeV for  $m_t = 170$  GeV,  $\alpha = 1/129$  and  $\Lambda_{\overline{MS}}^{(5)} = 225$  MeV in the NDR scheme [4].

NLO	$c_1$	$c_2$	$c_3$	$c_4$	$c_5$	$c_6$
$\mu = m_b/2$	1.137	-0.295	0.021	-0.051	0.010	-0.065
$\mu = m_b$	1.081	-0.190	0.014	-0.036	0.009	-0.042

these NLO wilson coefficients. The wilson coefficients  $c_i(\mu)$  and coupling constant  $\alpha_s(\mu)$  (in Eqn. (19)) are evaluated at  $\mu = m_b(m_b/2)$ . The scale chosen for the vertex, penguin, hard-spectator and annihilation term are described above (see the discussion before Eqn. (29)).

For the quark's constituent masses, we use  $m_b = 4.2$  GeV,  $m_c = 1.5$  GeV and  $m_s = 0.50$  GeV and  $m_u = m_d \sim 0.2$  GeV, the scale independent quantities [6, 7], which appear in the loop integral and for the current masses, we use their scale dependent values as listed in Table 3. which appear in the factorized

Table 3: The scale dependent current quark masses which are taken from [6],[7].

	$m_b(\mu)$	$m_s(\mu)$	$m_u(\mu)$	$m_d(\mu)$
$\mu = m_b/2$	4.88	0.122	$0.0413 \times m_s(\mu)$	$0.0413 \times m_s(\mu)$
$\mu = m_b$	4.20	0.090	$0.0413 \times m_s(\mu)$	$0.0413 \times m_s(\mu)$

amplitude after making the use of equation of motion of quarks.

The *decay constants* (in GeV) are given by ([6],[7])

$$f_B = 0.20, f_\pi = 0.131, f_K = 0.160, f_{\eta'}^c = 0.0058, f_\eta^c = 0.00093 \quad (32)$$

and we use  $f_0 = 1.10f_\pi$  and  $f_8 = 1.34f_\pi$  with the one angle mixing scheme (in  $\eta - \eta'$  sector) to obtain

$$f_\eta^u = \frac{f_8 \cos\theta}{\sqrt{6}} - \frac{f_0 \sin\theta}{\sqrt{3}}, \quad f_\eta^s = -2\frac{f_8 \cos\theta}{\sqrt{6}} - \frac{f_0 \sin\theta}{\sqrt{3}} \quad (33)$$

with  $\theta$ , the mixing angle, another unknown parameter in our analysis.

We use the following non-perturbative *form factors* values in our analysis [6],

$$\begin{aligned} F_{0,1}^{B \rightarrow \pi}(0) &= 0.28, \quad F_{0,1}^{B \rightarrow K}(0) = 0.34, \\ F_{0,1}^{B \rightarrow \eta}(0) &= F_0^{B \rightarrow \pi}(0) \left[ \frac{\cos\theta}{\sqrt{6}} - \frac{\sin\theta}{\sqrt{3}} \right]. \end{aligned} \quad (34)$$

For the distribution amplitudes (LCDA), we use the asymptotic form for the pseudoscalar mesons [6]

$$\Phi_\eta = 6x(1-x), \quad \Phi_K = 6x(1-x), \quad \text{twist} - 2 \text{ LCDA} \quad (35)$$

$$\Phi_\eta^{(3)} = 1, \quad \Phi_K^{(3)} = 1, \quad \text{twist} - 3 \text{ LCDA}. \quad (36)$$

The  $B$  meson wave function

$$\Phi_B(\bar{\rho}) = N_B \bar{\rho}^2 (1 - \bar{\rho})^2 \exp \left[ -\frac{1}{2} \left( \frac{\bar{\rho} m_B}{\omega_B} \right)^2 \right], \quad (37)$$

with the normalization constant  $N_B$  is being determined from the condition

$$\int_0^1 \Phi_B(\bar{\rho}) d\bar{\rho} = 1, \quad (38)$$

with  $m_B = 5.278$  GeV and  $\omega_B = 0.25$  GeV [11].

### 3.3 Results and Discussions

With all the numerical inputs in hand, we are now ready to discuss our results. Working within the QCD factorization framework, we made use of the  $BR(B^+ \rightarrow \eta K^+)$  and CP-asymmetry  $A_{cp}(B^+ \rightarrow \eta K^+)$  [8] data to obtain constraints in the  $\theta - \gamma$  plane. As we will see that the bound depends crucially on the scale  $\mu$  at which different nonfactorizable  $\mathcal{O}(\alpha_s)$  corrections are evaluated. The impact of the nonfactorizable *weak annihilation* correction, which is usually power suppressed, will also be considered while obtaining such constraints.

#### 3.3.1 Constraints in the $\theta - \gamma$ plane: with (without) the annihilation terms

We have seen that the effective coefficients  $a_i$ 's (Eqn.19), contains the wilson coefficients  $c_i$ 's, coupling constant  $\alpha_s(\mu)$  and several nonfactorizable corrections, which crucially depends on the renormalization scale  $\mu$ . For the wilson coefficients  $c_i$  in  $a_i$ , we use their NLO values for different  $\mu$  which are displayed in Table 2. The current quark mass which depends on the scale  $\mu$ , are displayed in Table 3. For the running coupling  $\alpha_s(\mu)$ , we use the oneloop expression for  $\alpha_s(\mu)$  as [10]

$$\alpha_s(\mu) = \frac{4\pi}{\beta_0 \text{Log} \left[ \mu^2 / \Lambda_{\overline{MS}}^2 \right]}, \quad (39)$$

where  $\beta_0 = \left( \frac{11}{3}N_c - \frac{2}{3}n_f \right)$  with  $N_c = 3$ , the colour and the typical QCD scale parameter  $\Lambda_{\overline{MS}}(\Lambda_{QCD}) = 226$  MeV with  $n_f = 5$ , the number of active quark flavour at  $\mu = m_b$  and similarly  $\Lambda_{\overline{MS}}(\Lambda_{QCD}) = 372$



MeV with  $n_f = 4$  for  $\mu = m_b/2$  [10]. Using these as inputs, we now use the BR and  $A_{cp}$  data ( Table 1) to obtain constraint in the  $\theta$  and  $\gamma$  plane. Before to obtain such constraints, let us see how the CP asymmetry  $A_{cp}$  varies with  $\gamma$  or  $\theta$ . In Figures 1(a,b) and 2(c,d), we made such plots. From Figures 1(a,b) ( standing respectively for  $\mu = m_b/2$  and  $m_b$  with the mixing angle  $\theta = -21.3^\circ$  [7]), we see that within the  $\pm 1\sigma$  deviation with respect to the the central value  $A_{cp}^{cen} = -0.25$ ,  $\gamma$  is allowed to varry in between  $+20^\circ$  and  $+100^\circ$  (one range),  $140^\circ$  and  $+170^\circ$  (other range). The negative  $\gamma$  is ruled out at the  $\pm 1\sigma$  level as far as the CP asymmetry data is concerned. From Figures 2(c,d), in which the unitarity angle  $\gamma$  is chosen as  $+70^\circ$  [6], the scale  $\mu$ , is being set at  $m_b/2$  and  $m_b$ , respectively, we find that at the  $\pm 1\sigma$  error away from the central value  $A_{cp}^{cen}$ , the mixing angle  $\theta$  is allowed to lie in between  $-45^\circ$  and  $-40^\circ$  (one range),  $-25^\circ$  and  $-10^\circ$  (other range). However, the  $A_{cp}$  data allows another region, in which  $\theta$  is positive. However, the constraints on  $\theta$ , which follows from the  $\eta \rightarrow \gamma\gamma$ ,  $\eta' \rightarrow \gamma\gamma$  and  $\pi^0 \rightarrow \gamma\gamma$  decay studies, suggest that  $\theta$  should be negaive i.e.

$$\theta = (-21.3 \pm 2.5)^\circ. \quad (40)$$

In order to have the overall consistency with other's analysis, we will not explore the *positive*  $\theta$  region. From the above analysis, where one angle is varied, while the other fixed, we know their sizes and signs. We will now explore the general possibility in which both  $\theta$  and  $\gamma$  is allowed to vary. In this case, by using the  $A_{cp}(B^+ \rightarrow \eta K^+)$  data, as well as the  $BR(B^+ \rightarrow \eta K^+)$  data, it is possible to constrain the two angles  $\theta$  and  $\gamma$  simultaneously by finding the contour plots in the  $\theta - \gamma$  plane.

In Figures 3(e, f), we obtain such contour plots corresponding to  $\mu = m_b/2$  and  $m_b$ . The central curve corresponds to the region allowed by the  $A_{cp} = -0.25$  (i.e. the central value), while the next(outer) to the central curve corresponds to  $A_{cp} = -0.11 (= -0.25 + 0.14)$  and the region between the outer and central curves, is allowed at the  $+1\sigma$  level. The innermost curve corresponds to  $A_{cp} = -0.39$  and the region between this curve and the central one, is allowed at the  $-1\sigma$  level. Note that a different set of  $\mu$  choice results into the change in the shape and hence the area of the allowed regions as a whole. At the  $\pm 1\sigma$  level, in either case, quite a large range of both  $\theta$  and  $\gamma$ 's are allowed: e.g. while the mixing angle  $\theta$  varies in between  $-42^\circ$  to  $-6^\circ$ , the unitarity angle  $\gamma$  can changes largely in between, say, e.g.  $10^\circ$  to  $175^\circ$  at the  $\pm 1\sigma$  level. As for example, say  $\gamma = 70^\circ$ , the contour plot suggest that  $\theta$  should lie in between  $-44^\circ$  and  $-40^\circ$  (left zone),  $-24^\circ$  and  $-6^\circ$  (right zone) for the scale  $\mu = m_b/2$ , while in between  $-42^\circ$  and  $-40^\circ$ (left zone),  $-26^\circ$  and  $-8^\circ$  (right zone) for the scale  $\mu = m_b$ .

In Figures 4(g, h), the  $\theta - \gamma$  contour plots corresponds to  $BR(B^+ \rightarrow \eta K^+) = (2.6 \pm 0.5) \times 10^{-6}$ . The renormalization scale  $\mu$  is chosen at  $m_b/2$  (Figure 4g) and  $m_b$  (Figure 4h). There are two regions in this plot. For each region, the central curve corresponds to the central value  $BR(B^+ \rightarrow \eta K^+) = 2.6 \times 10^{-6}$ , while the next(outer i.e. rightwards for the right side, and leftwards in the left side) to the central curve corresponds to  $BR(B^+ \rightarrow \eta K^+) = 3.1 \times 10^{-6}$  and the region between the outer and central curves (on either side), is allowed at the  $+1\sigma$  level. The two innermost curves corresponds to  $BR(B^+ \rightarrow \eta K^+) = 2.1 \times 10^{-6}$  and the region between this curve and the central one (in either side), is allowed at the  $-1\sigma$  level. The allowed contour region followed from the BR data, is rather narrow than that obtained from the  $A_{cp}$  data. Within  $\pm 1\sigma$  error bar, while  $\gamma$  can change widely in between  $0^\circ$  to  $180^\circ$ ,  $\theta$  changes very little: it change only by  $\pm 1^\circ$  with respect to the central value (corresponding to the central curve). Note that a different  $\mu$  shift the  $\theta - \gamma$  allowed contour region (see Figure 4g and 4h). As an example, say  $\gamma = 70^\circ$ , the contour plot suggest that  $\theta$  should lie in between  $-46^\circ$  and  $-44^\circ$  (left region) and in between  $-30^\circ$  and  $-26^\circ$  (right region) for the scale  $\mu = m_b/2$ , while for  $\mu = m_b$ , it lies in between  $-54^\circ$  and  $-50^\circ$  (left region) and  $-30^\circ$  and  $-26^\circ$  (right region).

To see the explicit scale dependence of the BR and CP asymmetry  $A_{cp}$  results, let us calculate them for some chosen  $\mu$  values. At  $\mu = m_b/2$ , with  $\theta = -21.3^\circ$  and  $\gamma = 70^\circ$ , a point well within the allowed region, we find  $BR(B^{-(+)} \rightarrow \eta K^{-(+)}) = 2.98(5.72) \times 10^{-6}$  and  $A_{cp}(B^- \rightarrow \eta K^-) = -0.315$  when the annihilation term is taken into consideration. If the annihilation term is switched off, the correponding predictions turns out to be  $BR(B^{-(+)} \rightarrow \eta K^{-(+)}) = 3.0(5.83) \times 10^{-6}$  (a change about 2%(11%)) and  $A_{cp}(B^- \rightarrow \eta K^-) = -0.319$  (a change of  $\sim 4\%$ ). Similarly, for  $\mu = m_b$ , with the same  $\gamma$  and  $\theta$  value and considering the the annihilation contribution, we find  $BR(B^{-(+)} \rightarrow \eta K^{-(+)}) = 2.93(4.91) \times 10^{-6}$  and  $A_{cp}(B^- \rightarrow \eta K^-) = -0.252$ . Without the annihilation term, we find  $BR(B^{-(+)} \rightarrow \eta K^{-(+)}) = 2.94(4.93) \times 10^{-6}$  (a change about 1%(2%)) and  $A_{cp}(B^- \rightarrow \eta K^-) = -0.253$  (a change of  $\sim 1\%$ ). So, the

impact of power correction (annihilation contribution) on  $BR$  and  $A_{cp}$  at different  $\mu$  is not so significant and consequently, in constraining the parameter space of  $\theta$  and  $\gamma$ .

In Figures 5(i, j) and 6(k, l), we have plotted  $A_{cp}$  and  $BR(B^+ \rightarrow \eta K^+)$  as a function of  $\theta$  and  $\gamma$  with different set of the renormalization scale i.e.  $\mu = m_b/2$  (left one) and  $m_b$  (right one). Note the differences arises due to the choice in renormalization scale: in Figures 5(i,j) larger negative  $A_{cp}$  may arise at  $\mu = m_b$  than that due to  $\mu = m_b/2$  and in Figures 6(k,l), in the same way large BR also arise at  $\mu = m_b/2$  in comparison to  $\mu = m_b$ . Finally, from the Figures 5(i, j), we see that a large negative  $A_{cp}$ , consistent with the present data, allows  $\theta$  to lie around  $-40^\circ$ , for a wide range of  $\gamma$ , consistent with our finding.

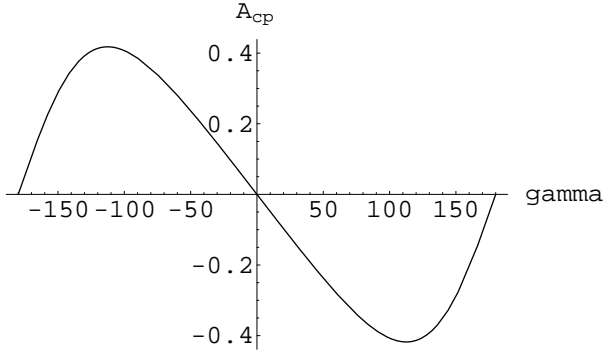
## 4 Summary and Conclusion

We have investigated the charmless nonleptonic  $B \rightarrow \eta K$  decay within the QCD factorization framework in the Standard Model. Two crucial things in the decay amplitudes are: (i) the unitarity angle  $\gamma$ , and (ii) the  $\eta - \eta'$  mixing angle  $\theta$ , which possesses several independent constraints followed from different studies. By knowing either  $\theta$  or  $\gamma$  from others analysis and using the HFAG  $A_{cp}$  data, one can get some idea about the allowed range of  $\gamma$  or  $\theta$ . We considered the most general scenario in which both  $\theta$  and  $\gamma$  are being treated as the unknown parameters. We use the  $BR(B^+ \rightarrow \eta K^+)$  and  $A_{cp}(B^+ \rightarrow \eta K^+)$  (available in the HFAG website) to constrain the  $\theta - \gamma$  contour plane. Using the  $A_{cp}$  data, at the  $\pm 1\sigma$  level, we found that when the angle  $\theta$  varies in between  $-42^\circ$  to  $-6^\circ$  (in two ranges), the angle  $\gamma$  can vary in between  $0^\circ$  to  $180^\circ$ . For the  $BR(B^+ \rightarrow \eta K^+) = (2.6 \pm 0.5) \times 10^{-6}$ , with  $\gamma = 70^\circ$ , we found that  $\theta$  can vary in between  $-46^\circ$  and  $-44^\circ$ ,  $-30^\circ$  and  $-26^\circ$  for  $\mu = m_b/2$ . For  $\mu = m_b$ , the corresponding allowed range is in between  $-54^\circ$  and  $-50^\circ$ ,  $-30^\circ$  and  $-26^\circ$  with the same choice of  $\gamma$ . We find the difference in the allowed contour region of  $\theta$  which follows from the  $A_{cp}$  and  $BR$  constraints, a crucial finding of the present study. We made our analysis for different set of renormalization scales i.e.  $\mu$ 's, which results into change in the allowed region in the  $\theta - \gamma$  contour plane. This is an important observation of this work. The effect of power correction correction is also investigated and found to be not so significant in constraining the  $\theta - \gamma$  contour plane. This is so because it's (power correction) impact on  $A_{cp}$  and  $BR(B^{-(+)} \rightarrow \eta K^{-(+)})$  are about 1% and 1%(2%), respectively.

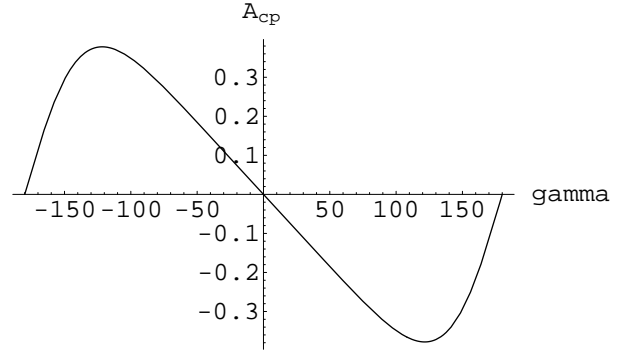
*Acknowledgments* I would like to thank the physics department of CYCU, Chung-Li, Taiwan (R.O.C) for the hospitality where a part of this work is being completed.

## References

- [1] R. Anastassov et al. (CLEO collaboration), CLEO CONF 97-24, EPS-334; B.H.Behrens et al. (CLEO collaboration), hep-ex/9801012.
- [2] B. Aubert *et al.* [BABAR Collaboration], Phys. Rev. D **69**, 031102 (2004); Phys. Rev. Lett. **93**, 231801 (2004).
- [3] J. Zhang *et al.* [BELLE Collaboration], Phys. Rev. Lett. **91**, 221801 (2003).
- [4] M. Beneke, G. Buchalla, M. Neubert and C. T. Sachrajda, Phys. Rev. Lett. **83** (2001) 1914; Nucl. Phys. B591 (2000) 313; Nucl. Phys. B606 (2001) 245.
- [5] M. Kobayashi, T. Maskawa, Progs. Theo. Phys. **45** (1973) 652.
- [6] M. Beneke and M. Neubert, Nucl. Phys. B675 (2003) 333.
- [7] A. Ali and C. Greub, Phys. Rev. D **57** (1998) 2996.
- [8] Heavy Flavor Averaging Group, <http://www.slac.stanford.edu/xorg/hfag/rare/index.html>: 2005.
- [9] Particle Data Group, Phys. Lett. B592 (2004) 1.
- [10] G. Buchalla, A. J. Buras and M. E. Lautenbacher, Rev. Mod. Phys. **68** (1996) 1125; A. J. Buras, hep-ph/9806471.
- [11] H. Y. Cheng and K. C. Yang, Phys. Lett. B511 (2001) 40.

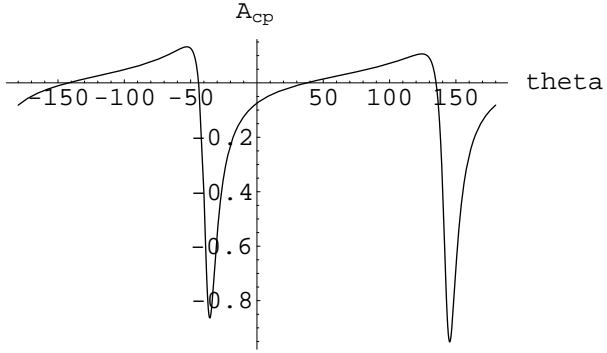


(a)

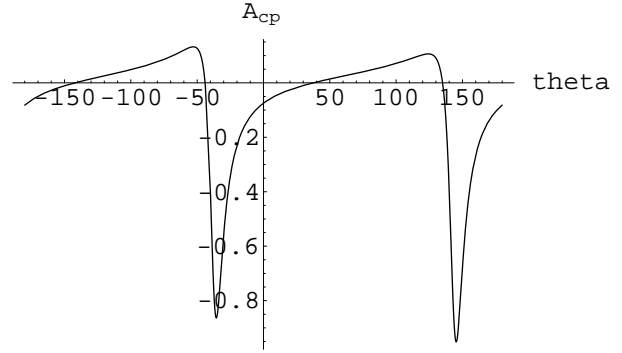


(b)

**Figure 1[a, b].** Plot showing the CP asymmetry  $A_{cp}(B^+ \rightarrow \eta K^+)$  as a function of the unitarity angle gamma ( $\gamma$ , given in degree). The most recent data [8] for  $A_{cp} = -0.25 \pm 0.14$ . The Figure 1a and 1b corresponds to the following choice of the renormalization scale:  $\mu = \frac{m_b}{2}$  (Fig.1a) and  $\mu = m_b$  (Fig.1b).

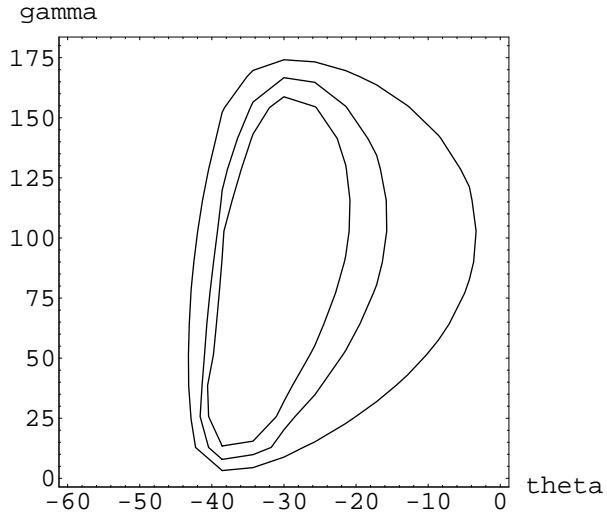


(c)

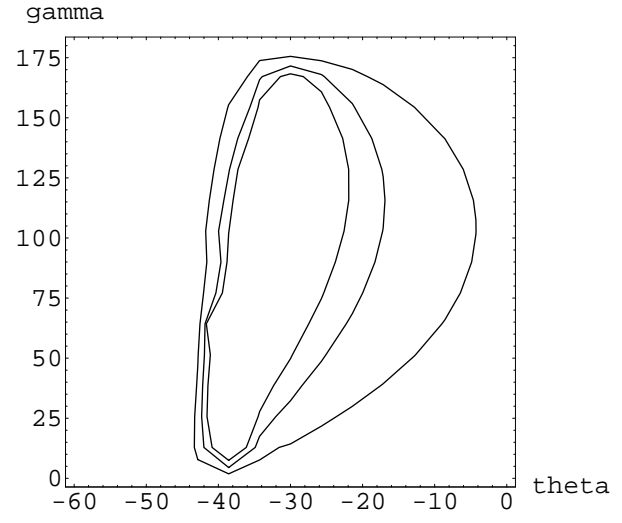


(d)

**Figure 2[c, d].** Plot showing the CP asymmetry  $A_{cp}(B^+ \rightarrow \eta K^+)$  as a function of the  $\eta$ - $\eta'$  mixing angle  $\theta$  ( $\theta$ , given in degree). The CP-asymmetry  $A_{cp} = -0.25 \pm 0.14$  according to the HFAG website [8]. The Figure 2c and 2d corresponds to the choice of the renormalization scale:  $\mu = \frac{m_b}{2}$  (Fig.2c) and  $\mu = m_b$  (Fig.2d).

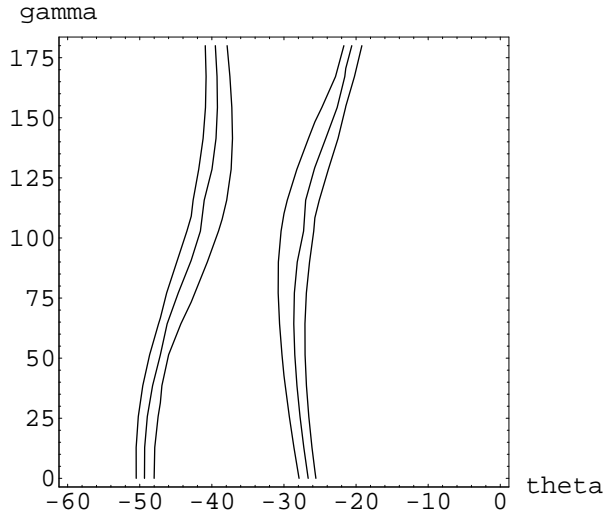


(e)

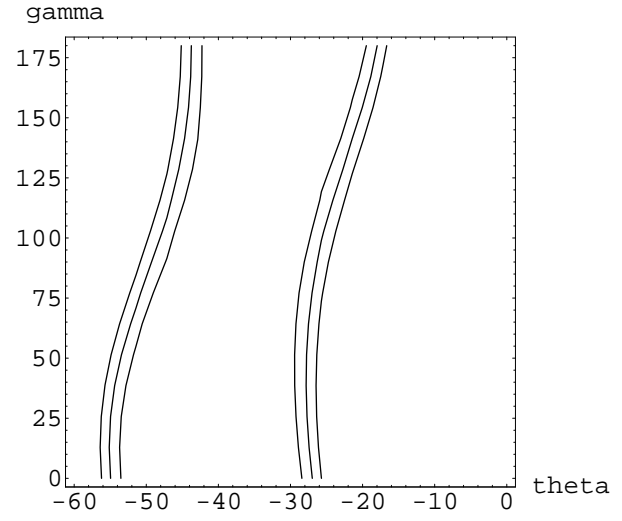


(f)

**Figure 3[e, f].** Contour plots in the theta ( $\theta$ ) - gamma ( $\gamma$ ) plane (angles are given in degree) using  $A_{cp} = -0.25 \pm 0.14$  [8] with the renormalization scale  $\mu = m_b/2$  (Fig.3e) and  $m_b$  (Fig.3f), respectively.

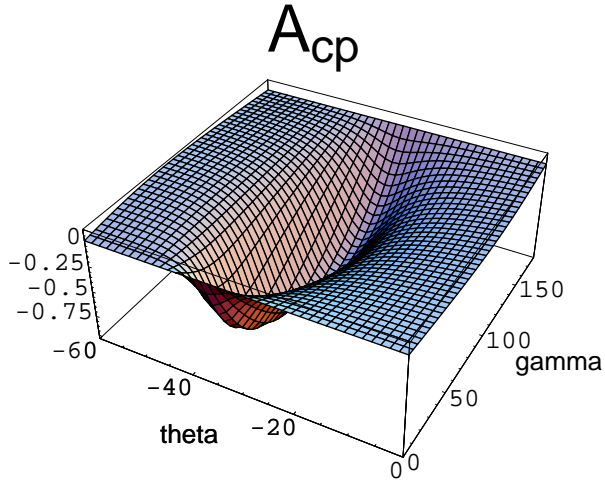


(g)

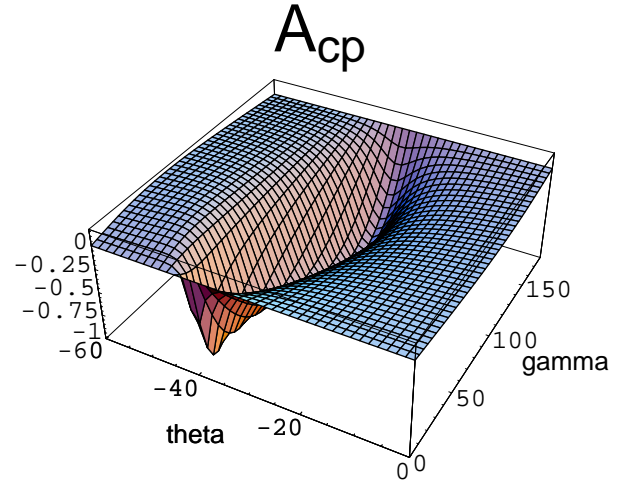


(h)

**Figure 4[g, h].** Contour plots in the  $\theta$  -  $\gamma$  plane (angles are given in degree) using  $BR(B^+ \rightarrow \eta K^+) = (2.6 \pm 0.5) \times 10^{-6}$  [8] with the renormalization scale  $\mu = m_b/2$  (Fig.4g) and  $m_b$  (Fig.4h), respectively.

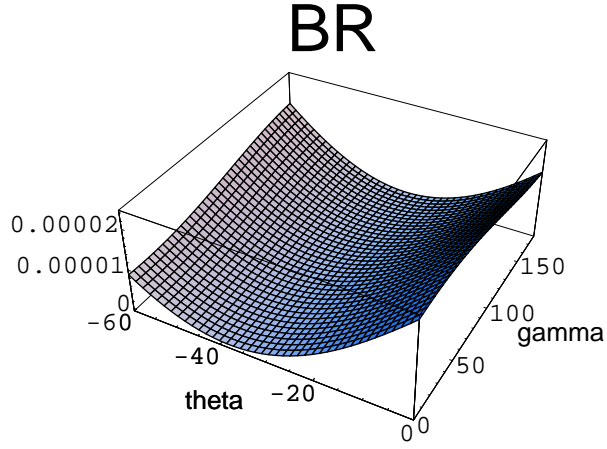


(i)

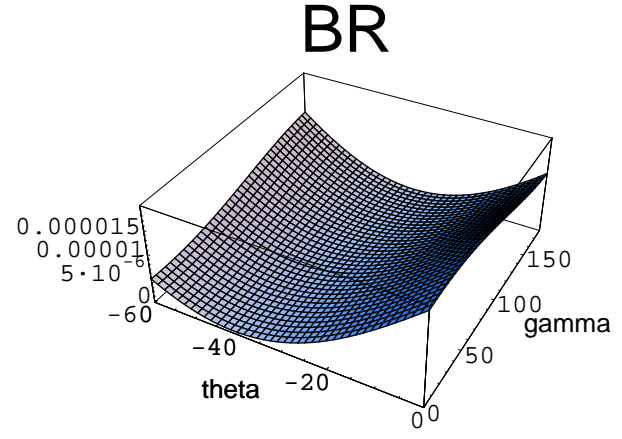


(j)

**Figure 5[i, j].** Showing the CP-asymmetry  $A_{cp}(B^+ \rightarrow \eta K^+)$  as a function of the mixing angle  $\theta$  and the unitarity angle  $\gamma(\gamma)$ . The angles are given in degree. The left one corresponds to the renormalization scale  $\mu = m_b/2$  (Fig.5i), whereas the right one,  $\mu = m_b$  (Fig.5j).



(k)



(l)

**Figure 6[k, l].** Showing the  $BR(B^+ \rightarrow \eta K^+)$  as a function of the mixing angle  $\theta$  (degree) and the unitarity angle  $\gamma$  (degree). The angles are in degree. The left one corresponds to the renormalization scale  $\mu = m_b/2$  (Fig.6k), whereas, the right one,  $\mu = m_b$  (Fig.6l).